Subduction of the Philippine Sea plate beneath southwestern Japan: Slab geometry and its relationship to arc magmatism

Junichi Nakajima[1] and Akira Hasegawa[1]

[1]   We carry out high-resolution three-dimensional seismic tomography of the crust and upper mantle beneath southwestern (SW) Japan using arrival-time data obtained from the nationwide seismograph network. The tomographic images provide new insights into the configuration of the Philippine Sea slab and arc magmatism. The results confirm the existence of an aseismic portion of the Philippine Sea slab at greater depths beyond the seismic portion. The Philippine Sea slab is subducting aseismically down to at least a depth of 200 km in Chubu, 60–80 km in Kinki, and 60 km in Chugoku and is subducting seismically to depths of 150–200 km in Kyushu. In the Chubu district, it is subducting seismically at a shallow dip and then bends downward beneath the volcanic area, whereas in the Kinki district, it is subducting subhorizontally as far as the Japan Sea. The differences in the slab geometry between adjacent regions correlate with the differences in volcanic activity, suggesting the importance of the geometry of the Philippine Sea slab on arc magmatism. Our tomographic images further imply subduction of the Philippine Sea slab down to a depth of around 70 km northwest of the Izu Peninsula. The Philippine Sea slab in that region might have split into western and eastern parts separated by a slab tear and collided with the Pacific slab at depths of 150–200 km.

1.   Introduction

[2]   Subduction zones are locations where the oceanic slab subducts into the mantle. The subduction process induces mantle convection and causes geophysical and geochemical heterogeneity in the mantle. Magmatism, which is a major contributor to the growth of new continental crust, is one of the most striking features resulting from the subduction of the oceanic slab. Magmatism and its surface manifestation depend largely on the geometry of the subducted slab; therefore the configuration of the subducted slab is of considerable importance in understanding the tectonic framework of subduction zones.

[3]   In southwestern (SW) Japan, the Philippine Sea plate subducts along the Sagami and Nankai troughs with a subduction velocity of 3 to 5 cm/yr, and the Pacific plate subducts along the Japan and Izu-Bonin trenches with a subduction velocity of ∼8 cm/yr [e.g., *Seno et al.*, 1996]. The Philippine Sea plate is divided into three north-south trending regions according to formation age. The eastern part, including the Izu-Bonin arc, formed before 40 Ma; the central part, the Shikoku basin, formed as a back-arc basin during 27 to 15 Ma [*Okino et al.*, 1994]; and the western part, comprising several old ridges and basins, is older than 50 Ma [e.g., *Tokuyama*, 1995] (Figure 1a). Subduction of

the Philippine Sea slab at the Sagami trough and the eastern end of the Nankai trough has caused a collision of the Izu-Bonin volcanic ridge with central Japan, forming an Izu collision zone [*Soh et al.*, 1998].

[4]   As a result of subduction of the Philippine Sea slab, a large number of large earthquakes have occurred in the overriding plate, along the plate interface, and within the slab. The Nankai (M8.0) and Tonankai (M8.1) earthquakes occurred in 1944 and 1946, respectively, along the plate interface, and the Geiyo earthquake (M6.7) occurred in 2001 within the slab. Two large earthquakes, the Kobe earthquake (M7.2) and the western Tottori earthquake (M7.3), occurred in the overriding plate. These earthquakes caused severe damage to urban areas. The estimated source areas of the next major Nankai, Tonankai, and Tokai earthquakes [*Headquarters for Earthquake Research Promotion*, 2001] are along the Nankai trough (Figure 1b). *Obara* [2002] found that non-volcanic deep tremors have occurred in SW Japan along the strike of the Philippine Sea slab over a length of 600 km. The tremors are distributed at the downdip limit of the source areas of these three large interplate earthquakes (Figure 1b). Short- and long-term slow slip events correlated with the major migrating tremor activity have been detected in the Bungo channel [e.g., *Hirose and Obara*, 2005] and the Tokai district [*Ozawa et al.*, 2002]. These events are considered to be closely associated with the subduction of the Philippine Sea slab. Besides understanding the tectonic framework in SW Japan, a detailed configuration of the Philippine Sea slab is

[1]Research Center for Prediction of Earthquakes and Volcanic Eruptions, Graduate School of Science, Tohoku University, Sendai, Japan.
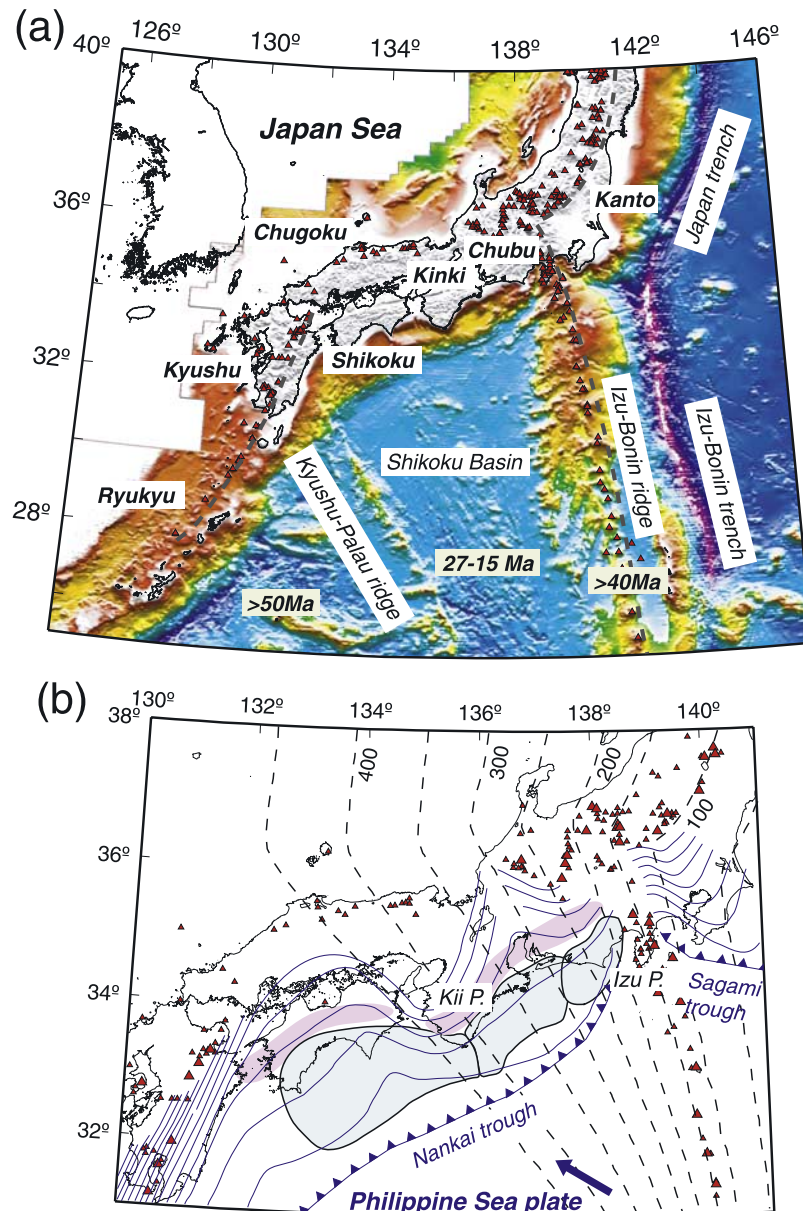
Figure 1. (a) Morphology around the Japanese Islands. Red triangles denote the active and Quaternary volcanoes [*Committee for Catalog of Quaternary Volcanoes in Japan*, 1999]. Gray broken curves represent the volcanic front. The formation age of the Philippine Sea slab varies along the arc [e.g., *Okino et al.*, 1994; *Tokuyama*, 1995]. (b) The isodepth contours of the Pacific slab [*Zhao and Hasegawa*, 1993; *Nakajima and Hasegawa*, 2006] are shown by broken curves with an interval of 50 km, while those of the compromised model of the Philippine Sea slab [*Wang et al.*, 2004] are shown by blue curves with an interval of 10 km. Troughs are shown by serrated lines. The blue arrow represents the plate motions of the Philippine Sea slab relative to the Eurasian plate [*Seno et al.*, 1996]. The spatial distribution of nonvolcanic deep tremors [*Obara*, 2002] is shown by pink belts. The estimated source areas of the next major Nankai, Tonankai, and Tokai earthquakes are represented by light blue hatches [*Headquarters for Earthquake Research Promotion*, 2001]. Large and small red triangles denote active and Quaternary volcanoes, respectively.

essential to constrain the factors controlling the occurrence of these earthquakes.

[5] Various models of the configuration of the Philippine Sea slab have been proposed on the basis of the distribution of seismicity and focal mechanisms [e.g., *Ishida*, 1992; *Nakamura et al.*, 1997; *Miyoshi and Ishibashi*, 2004; *Toda et al.*, 2005; *Hori*, 2006; *Wang and Zhao*, 2006a], distribution of repeating earthquakes [*Kimura et al.*, 2006], seismic velocity structures [e.g., *Sekiguchi*, 2001; *Matsubara et al.*, 2005], receiver function analyses [e.g., *Shiomi et al.*, 2004;
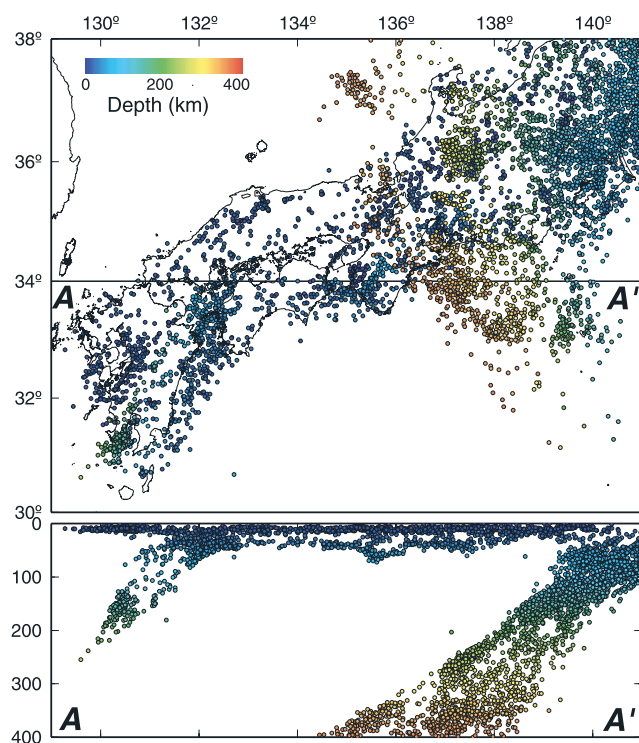
Figure 2. Distribution of 6187 events used in this study. Colors represent the depth of hypocenters. Hypocenters in the cross section are projected onto the A-A′ in the map.

Yamauchi et al., 2003; *Ramesh et al.*, 2005], waveform analyses [e.g., *Nakanishi*, 1980; *Oda and Douzen*, 2001], and reflection/refraction surveys [e.g., *Baba et al.*, 2002; *Sato et al.*, 2005]. *Wang et al.* [2004] proposed a compromised model of the Philippine Sea slab on the basis of these previous models (Figure 1b). However, the differences among the models are relatively large, and the configuration of the Philippine Sea plate is still debatable. The differences among the models are attributable to the differences in the method. Moreover, there is no model that specifies the configuration of the Philippine Sea slab for all of SW Japan.

[6] This paper describes a detailed velocity structure of the crust and the uppermost mantle beneath SW Japan in order to improve our understanding of the subduction of the Philippine Sea slab. It is the first attempt to propose a complete configuration of the Philippine Sea slab subducted from the Nankai trough, extending from Chubu to Kyushu. We applied traveltime tomography to available arrival-time data obtained from the Japan University Network Earthquake Catalog (JUNEC), the unified catalog by the Japan Meteorological Agency (JMA), and arrival-time data picked by Tohoku University. The Philippine Sea slab also subducts beneath the Kanto district from the Sagami trough (Figure 1b), and many models of the geometry of the Philippine Sea plate have been proposed on the basis of recent high-quality seismic data [e.g., *Matsubara et al.*, 2005; *Sato et al.*, 2005; *Toda et al.*, 2005; *Hori*, 2006; *Kimura et al.*, 2006]. Therefore, the configuration of the Philippine Sea slab beneath the Kanto district is beyond the main scope of this study. However, we will briefly include it

in our discussion in section 4 of the Philippine Sea slab in the northern region of the Izu collision zone.

2. Data and Method

[7] The number of seismograph stations in the Japanese Islands has remarkably increased since October 2000 because of the construction of high sensitive seismograph network Japan (Hi-net) by the National Research Institute for Earth Science and Disaster Prevention [*Okada et al.*, 2004], forming a dense nationwide seismograph network with a station separation of about 20 km. We used the arrival-time data of earthquakes in the period January 2001 to April 2006. The earthquakes used in this study were selected on the basis of the following criteria. First, the earthquakes with more than 20 arrival-time data were selected. Then, we selected one earthquake with the largest number of arrival-time data in each block by dividing the study area into $0.02° \times 0.02° \times 5$ km blocks, which yields the distribution of earthquakes in the study area as uniformly as possible. In this manner, 3608 earthquakes with focal depths <200 km and 456 earthquakes with focal depths >200 km were selected. We picked the arrival times of these earthquakes and obtained 493,591 P and 298,334 S wave arrival times.

[8] Two additional sets of arrival-time data for earthquakes with depths >200 km were used to constrain the deep structure and the thickness of the Philippine Sea slab. The first data set consists of 853 earthquakes recorded by the JMA in the period October 1997 to December 2000. The arrival times recorded by the JMA were used for these events (21,285 P and 11,576 S wave arrivals). The second data set consists of 1270 earthquakes from January 1992 to September 1997. The arrival-time data summarized in the JUNEC catalog were used for these events (47,270 P and 15,899 S wave arrivals). Figure 2 shows the distribution of 6187 earthquakes used in this study. Seismograph stations used in this study belong to the nationwide seismograph network, and the total number of stations is ∼1200 (Figure 3). The spatial separation of the stations is about 20 km. All the stations are equipped with three-component seismometers. The phase picking accuracy is $0.05-0.1$ to $0.1-0.2$ s for P and S wave arrivals, respectively.

[9] We applied the tomographic method [*Zhao et al.*, 1992a, 1994] to 562,146 P wave and 325,809 S wave high-quality arrivals from 6187 local earthquakes to determine the three-dimensional P and S wave velocity structures. We adopted the simplified velocity structure by *Ueno et al.* [2002], which is used in the routine work of the JMA, as an initial model for the P wave velocity. A constant Vp/Vs value of 1.73 was used to calculate an initial S wave velocity model. The crustal discontinuities (the Conrad and Moho) and the upper boundary of the subducted Pacific plate [*Zhao et al.*, 1992b; *Zhao and Hasegawa*, 1993; *Nakajima and Hasegawa*, 2006] were adopted in the inversion. In the initial model, we assigned P and S wave velocities within the subducted Pacific slab to be 5% faster than those in the mantle. To calculate traveltimes and raypaths accurately and rapidly, we employed the three-dimensional ray-tracing technique of *Zhao et al.* [1992a]. The principle of the ray-tracing scheme is to use the pseudo-bending algorithm [*Um and Thurber*, 1987] and Snell's low iteratively to perturb an initial ray until the raypath with the
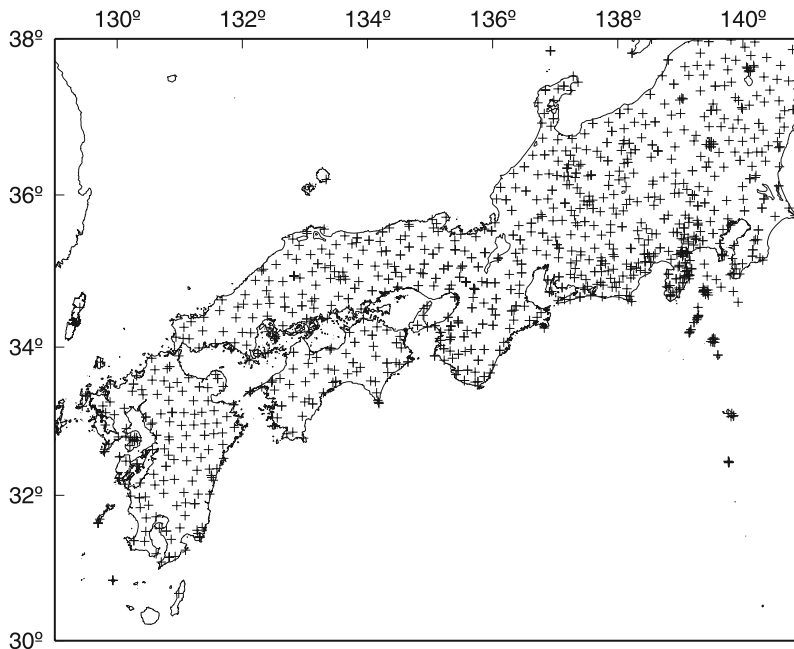
Figure 3. Distribution of the seismograph stations used in this study.

smallest traveltime is found. The nonlinear tomographic problem was solved by iteratively conducting linear inversions. In each iteration, perturbations to hypocentral parameters and velocities were determined simultaneously. The iterations were terminated when the reduction of the root mean square (RMS) of the arrival-time residuals converged. Further details of the method are given by *Zhao et al.* [1992a]. The hypocenters of all earthquakes were relocated using the initial one-dimensional velocity model before the three-dimensional inversion.

[10] For the model space, we considered the latitude range of $30°-38°$N, longitude range of $129°-141°$E, and depth range of $0-450$ km. We set the horizontal grid nodes with a spacing of $0.25°$ and $0.3°$ in the latitude and longitude directions, respectively, except for the Chugoku and Shikoku districts where the seismic activity associated with the subducted Philippine Sea slab is not high, and hence horizontal grid nodes with a spacing of $0.3°$ and $0.4°$ were adopted in the latitude and longitude directions, respectively (Figure 4a). Grid nodes were spaced vertically at $10-15$ km for depths <60 km and $20-40$ km for greater depths (Figure 4b). The seismic Philippine Sea slab is subducting down to depths of $\sim$60 km beneath Chubu, Chugoku, and Shikoku [e.g., *Nakamura et al.*, 1997], and dense grid nodes were set in the vertical direction for the corresponding depths. We carried out several sets of inversions and resolution tests with different grid intervals and found that the grid intervals smaller than the above mentioned ones lead to inaccurate tomographic images. The final results were obtained after five iterations. The RMS of
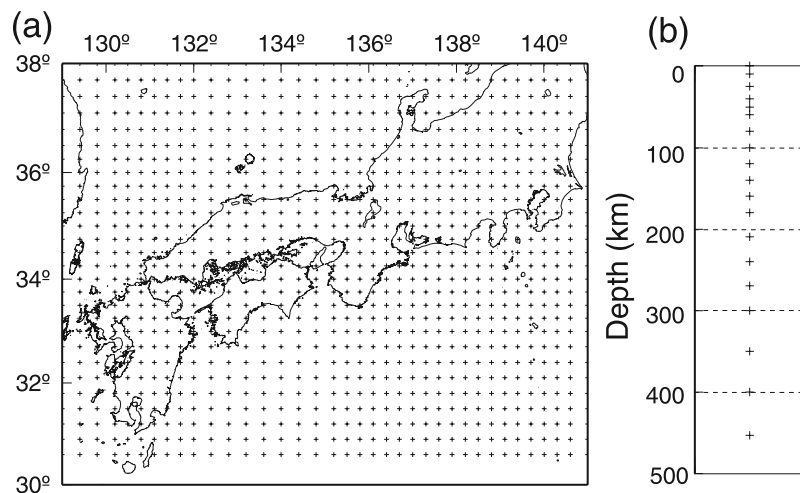

Figure 4. (a) Map and (b) cross-sectional views of the configuration of grid nodes adopted in the inversion. Grid spacing in the horizontal direction is $0.25°-0.4°$. Grid nodes are set up at depths of 0, 10, 25, 40, 50, 60, 80, 100, 120, 140, 160, 180, 210, 240, 270, 300, 350, 400, and 450 km.

residuals for the initial model, which were 0.50 s for the *P* wave and 0.72 s for the *S* wave, were reduced to 0.33 s and 0.52 s, respectively, upon optimization.

3. Results and Resolution Tests

[11] We carried out checkerboard resolution tests (CRTs) to ascertain the adequacy of ray coverage and the reliability of the obtained images. In the CRTs, positive and negative velocity perturbations of 6% were alternately assigned to the grid nodes along both the horizontal and vertical directions, and the traveltimes for this model were calculated to generate synthetic data. Synthetic data were constructed from the same source-receiver geometry as the observations with random noises corresponding to phase-picking errors (a standard deviation of 0.1 s for the *P* wave and 0.15 s for the *S* wave). Then, we inverted the calculated synthetic traveltime data using an initial model without any velocity anomalies.

[12] Figure 5 shows the map with the results of the CRTs at depths of 40, 60, 80, and 100 km. The results exhibit a good resolution beneath central Japan and Kyushu at all depths. The checkerboard patterns beneath the Chugoku and Shikoku districts are well recovered for the *P* waves but slightly smeared for the *S* waves along the coastline of the Japan Sea at depths >60 km. This is probably due to the insufficient number of raypaths. In the vertical cross sections shown hereafter, the conventional presentation of the results of the CRTs is not appropriate since the vertical cross sections shown are not parallel to the grid nodes adopted in the tomographic inversion. Hence we defined the "recovery rate of CRTs." The rate of the inverted (recovered) velocity perturbations with respect to the input (correct) velocity perturbation assigned in the model for the calculation of synthetic traveltime data is calculated for each grid node. Positive and negative signs mean that the inverted (recovered) velocity perturbation shows signs that are the same and opposite to those of the input (correct) ones. Thus 100% indicates complete resolution for that grid. We calculate the recovery rate of the CRTs and show it for the cross sections discussed hereafter. We also conducted restoring resolution tests (RRTs) [*Zhao et al.*, 1992a] on the obtained structure. The methods of ray tracing and inversion are the same as those in the CRTs. The results of the RRT demonstrate the reliability of the obtained images of the region beneath the land area.

[13] Figure 6 shows the map showing the *P* and *S* wave velocity perturbations at depths of 40, 60, 80, and 100 km. To remove the dependence of the inversion results on the grid configuration shown in Figure 4, we carried out three more inversions with three grid configurations shifted by half a grid interval toward the northeast, depth, and northeast and depth directions, and calculated the average values of the inverted velocity at each grid node. The results shown hereafter are the average values derived from four inversions with different grid configurations. The velocity structures are shown only for regions with >100 raypaths, where the checkerboard patterns are recovered well, and hence the obtained velocity structures are reliable.

[14] At a depth of 40 km, a distinct E-W trending low-velocity zone exists beneath Kanto. *Matsubara et al.* [2005] interpreted the low-velocity zone to be the oceanic crust of

the subducted Philippine Sea slab. Another prominent low-velocity zone is the north of the Izu Peninsula. An *S* wave low-velocity zone is detected along the coastline of the Japan Sea in the Chugoku district. The low-velocity zone coincides spatially with the helium volcanic front [*Sano et al.*, 2006] and the Quaternary volcanic front [*Kimura et al.*, 2005]. The fore-arc side of the mantle wedge beneath Kyushu exhibits low-velocity anomalies for *P* and *S* waves, consistent with the results of previous studies [*Zhao et al.*, 2000; *Honda and Nakanishi*, 2003; *Wang and Zhao*, 2006b]. Deep low-frequency earthquakes [*Obara*, 2002; *Katsumata and Kamaya*, 2003] occur in and around the *S* wave low-velocity zone beneath Chubu, the Kii Peninsula, and the central to western part of Shikoku. A high-velocity anomaly exists in the eastern Shikoku, where no deep low-frequency earthquakes occur. Note the absence of deep low-frequency earthquakes in the fore-arc side of Kyushu despite the existence of a prominent low-velocity zone. A high-velocity anomaly, particularly for *S* waves, is imaged from Chubu to Kyushu along the coastline of the Pacific Ocean, which corresponds to the subducted Philippine Sea slab.

[15] A high-velocity anomaly interpreted to be the subducted Philippine Sea slab extends northward at a depth of 60 km from the Chubu to Shikoku districts. A prominent low-velocity zone is detected beneath the volcanic area in central Japan. Low-velocity zones are also distributed near the coastline of the Japan Sea and in the back-arc side of Kyushu. Beneath Kyushu, a high-velocity zone exists in the fore-arc side at a depth of 80 km, which corresponds to the subducted Philippine Sea slab. A distinct low-velocity zone, particularly for *S* waves, is imaged from Chubu to the east of Shikoku, which is also visible at deeper depths. These low-velocity zones are located below the Philippine Sea slab. At deeper depths, a high-velocity anomaly corresponding to the Philippine Sea slab exists only in central Japan and Kyushu.

4. Discussion

4.1. Configuration of the Philippine Sea Slab

[16] The subduction of the Philippine Sea slab has been modeled chiefly by the distribution of Wadati-Benioff zone seismicity and seismic reflection/refraction surveys. It is known that the Philippine Sea slab is subducting seismically to depths of 40–80 km beneath Chubu, Kinki, and Chugoku and 150–180 km beneath Kyushu [e.g., *Nakamura et al.*, 1997; *Goto et al.*, 2001; *Miyoshi and Ishibashi*, 2004]. Recent analyses of the receiver function and later phases have suggested the existence of the aseismic Philippine Sea slab at a deeper extension of the seismic slab [e.g., *Nakanishi et al.*, 2002; *Yamauchi et al.*, 2003; *Shiomi et al.*, 2004; *Ramesh et al.*, 2005]. The subduction of the aseismic Philippine Sea slab has been partly constrained by seismic tomography [*Sekiguchi*, 2001; *Nakamura et al.*, 2002; *Honda and Nakanishi*, 2003; *Zhao et al.*, 2004]. For example, the aseismic Philippine Sea slab is traced down to a depth of 60 km beneath the Chugoku district where the subduction of the seismic slab is confined to depths shallower than 40 km. Although the subduction of the aseismic Philippine Sea slab has been recognized, a configuration of the Philippine Sea slab for the entire SW Japan has not yet been understood.
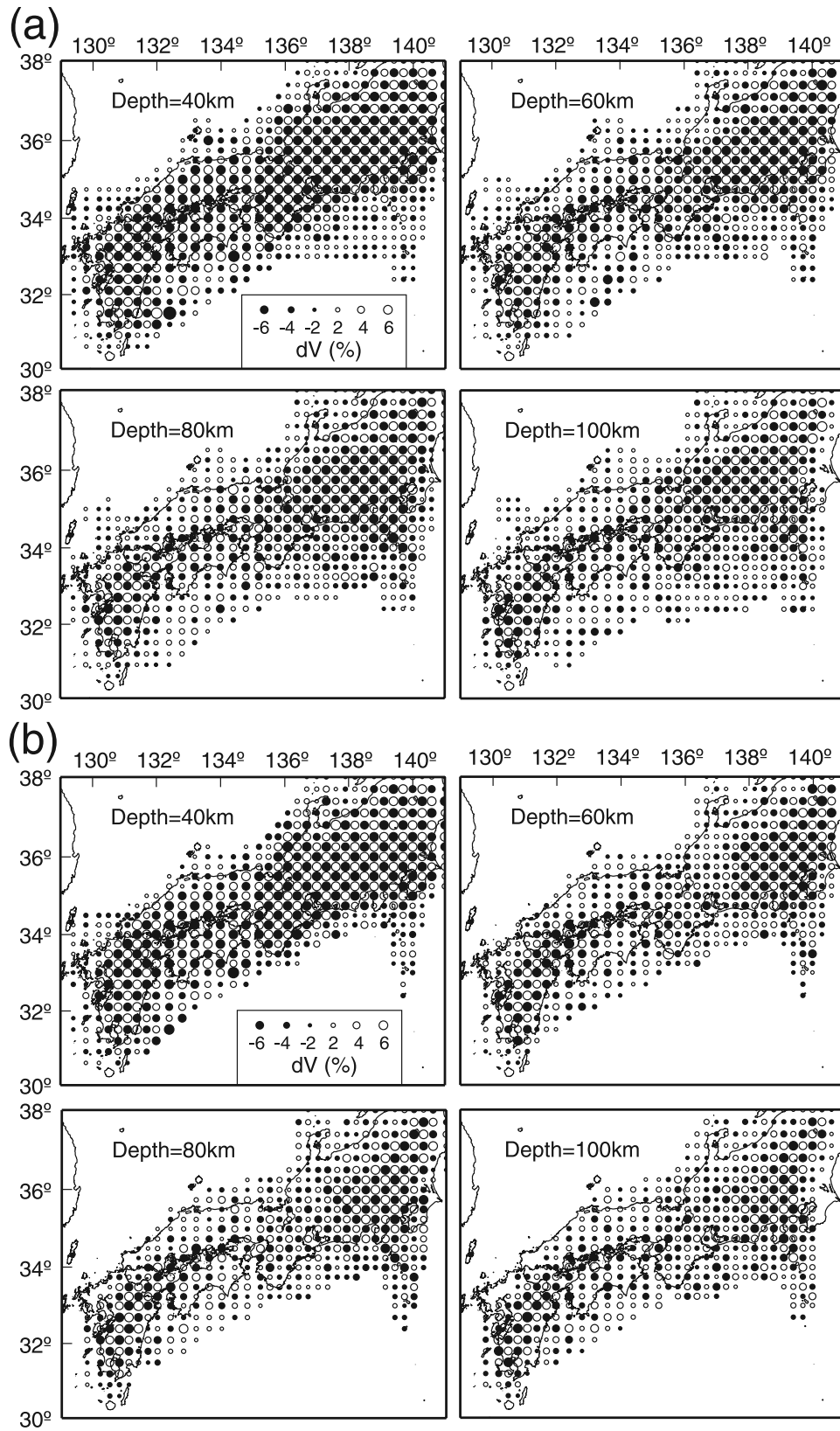
Figure 5. Results of the checkerboard resolution tests of (a) *P* wave and (b) *S* wave for four representative depth layers. Solid and open circles denote low and high velocities, respectively.
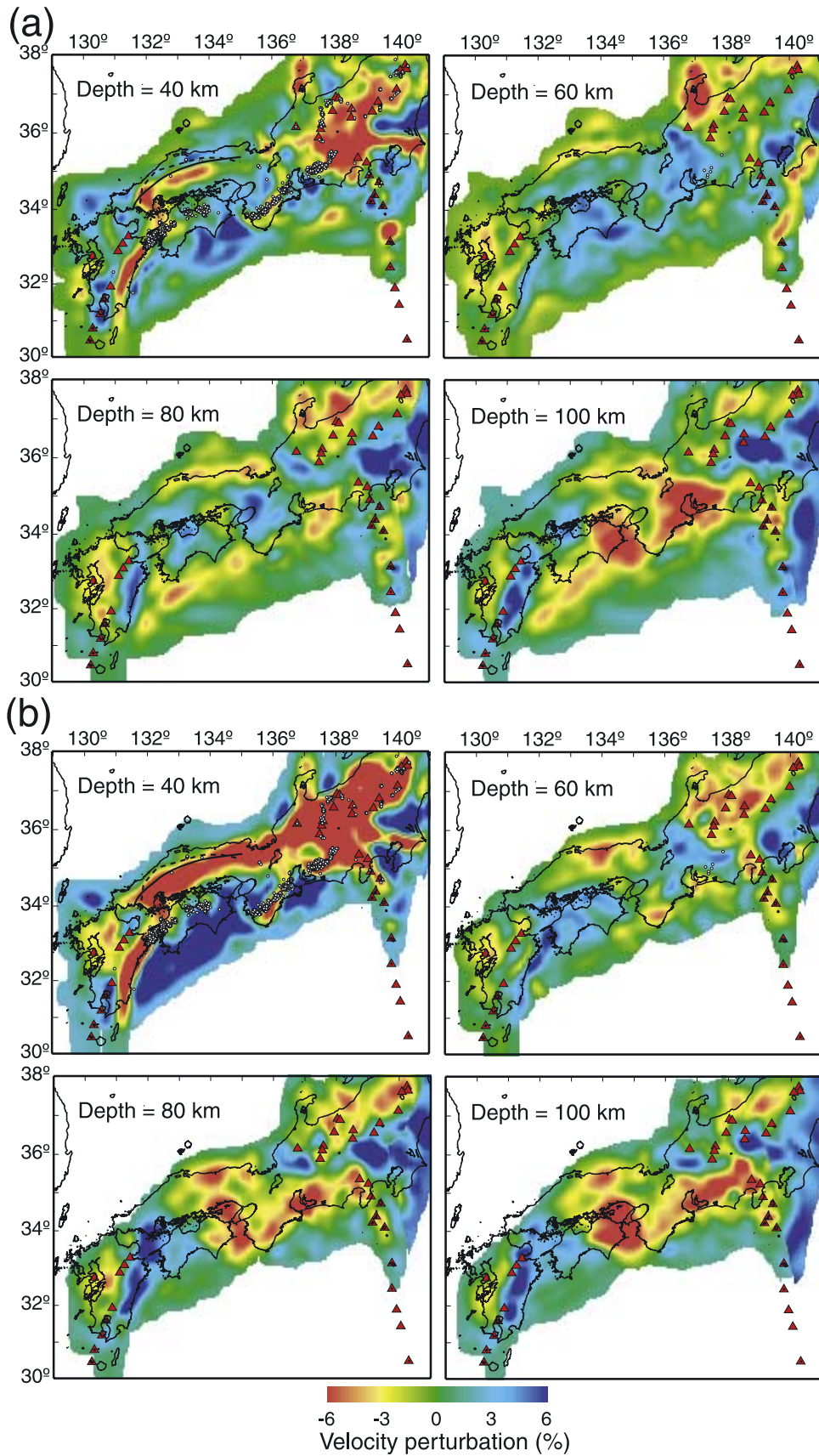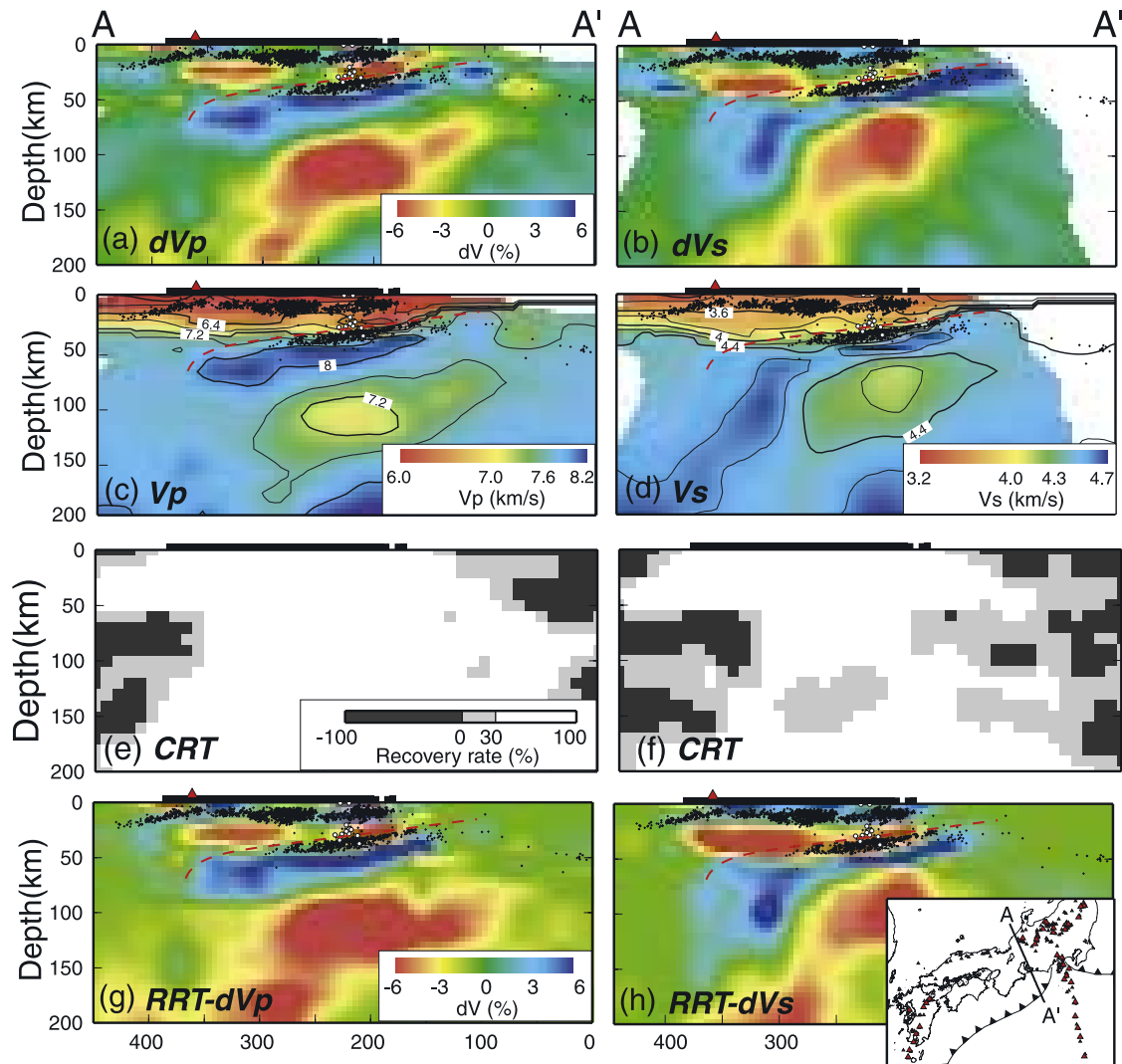
Figure 6

Figure 7. Across-arc vertical cross sections of (a) *P* wave and (b) *S* wave velocity perturbations, (c) *P* wave and (d) *S* wave absolute velocities, the recovery rate of CRTs for (e) *P* and (f) *S* waves, and results of RRT for (g) *P* and (h) *S* waves along the profile, A-A′, in the insert map. The red curve in each figure denotes the upper interface of the subducted Philippine Sea slab inferred from the seismicity and velocity structures. Crosses and white circles show microearthquakes and deep low-frequency earthquakes within a 10-km wide zone along the profile. Black bars and red triangles on the top of each figure denote the land area and Quaternary volcanoes, respectively. The regions with the number of rays >100 are shown in Figures 7a–7d.

[17] We propose a new configuration of the Philippine Sea slab on the basis of the seismic velocity structures obtained in this study. Figure 7 depicts the vertical cross sections of *P* and *S* wave velocity perturbations and absolute velocities along the line in the insert map. Figures 7a and 7b show that earthquakes occur along a NW-dipping plane at depths between 20 to 50 km, which corresponds to the seismicity related to the Philippine Sea slab subducted from the southeast. We use the upper envelope of the slab seismicity to infer the upper boundary of the subducted Philippine Sea slab since the majority of earthquakes within the Philippine Sea slab are considered to occur in the oceanic crust [*Hori et al.*, 1985; *Ohkura*, 2000]. At greater depths, the seismicity associated with the Philippine Sea slab is absent and the velocity structure is the only indication of the location of the Philippine Sea slab. A high-

Figure 6. The distribution of (a) *P* wave and (b) *S* wave velocity perturbations (in %) of 40, 60, 80, and 100 km. The red and blue colors denote low and high velocities, respectively. The perturbation scale is shown at the bottom. Red triangles represent active volcanoes. White circles represent the distribution of deep low-frequency earthquakes reported by the JMA. The regions with the number of rays >100 are shown. Dashed and solid curves shown in the result of a depth of 40 km represent the Quaternary [*Kimura et al.*, 2005] and helium volcanic fronts [*Sano et al.*, 2006], respectively.

velocity zone for both *P* and *S* waves continues from the seismic Philippine Sea slab to a depth of 70 km. The absolute *P* wave velocity is approximately 8.0 km/s (Figure 7c), comparable to those expected for the slab mantle from the reflection/refraction surveys [e.g., *Iidaka et al.*, 2003; *Kodaira et al.*, 2004]. The results of the CRTs show a good recovery in the regions of the high-velocity anomaly (Figures 7e and 7f), and those of RRT also demonstrate that the high-velocity anomaly is well restored (Figures 7g and 7h). Therefore we consider that the high-velocity zone downdip of the subducted seismic Philippine Sea slab is the aseismic portion of the Philippine Sea slab, and we delineate the upper boundary of the Philippine Sea slab along the upper boundary of the high-velocity zone. The continuity of the high-velocity zone between adjacent cross sections is also taken into consideration to delineate the configuration of the Philippine Sea slab.

[18] The inferred upper boundary of the subducted Philippine Sea slab is indicated by a red broken curve in Figure 7. The Philippine Sea slab is aseismically subducting to a depth of 70 km and almost reaches the coastline of the Japan Sea. The thickness of the Philippine Sea slab is estimated to be 30 km, in agreement with previous studies [e.g., *Ishida*, 1992; *Matsubara et al.*, 2005]. It is difficult to image the Philippine Sea slab for depths shallower than 20 km because of the limited ray coverage and resulting low resolution; the configuration of the Philippine Sea slab at these depths is based on the results of the reflection/refraction surveys [e.g., *Baba et al.*, 2002].

[19] Figure 8 shows the vertical cross sections of *P* and *S* wave velocity perturbations along four profiles in the inset map. It is likely that the subducted Philippine Sea slab is complicated, with along-arc variations in its depth and dip. Slab seismicity occurs down to a depth of 50 km in Figure 8a, and the high-velocity zone, particularly for the *S* wave, is imaged to depths of ~200 km. As the resolution is good in the region where the high-velocity zone is imaged, we consider that relatively weak amplitude of the high-velocity anomaly is reliable. The subduction of the aseismic Philippine Sea slab in this region was partly revealed by *Sekiguchi* [2001] and *Nakamura et al.* [2002]. The subduction of the Philippine Sea slab down to a depth of ~200 km in central Japan could account for the distribution of volcanoes and other geophysical observations, as discussed later.

[20] The Philippine Sea slab is not imaged as a high-velocity zone along line B-B′ (Figure 8b), which crosses the Kii Peninsula. The checkerboard patterns are well recovered beneath the land area, and they demonstrate the reliability of the obtained velocity structures. The absence of the high-velocity zone corresponding to the subducted Philippine Sea slab has been known to be a unique feature beneath the Kii Peninsula [*Seno et al.*, 2001; *Honda and Nakanishi*, 2003; *Salah and Zhao*, 2003]. Recently, *Nakajima and Hasegawa* [2007] have revealed the existence of a large upwelling flow below the Philippine Sea slab around the Kii Peninsula. This flow appears to partly penetrate the subducted Philippine Sea slab beneath the Kii Peninsula. They argued that the Philippine Sea slab might be more hydrated than the surrounding regions as a result of its interaction with the upwelling; serpentinization of the slab mantle could have lowered the seismic velocity within the slab. Therefore in this study, we referred only to the distribution of a NW-dipping seismicity to delineate the slab geometry beneath the Kii Peninsula.

[21] It is argued that the Philippine Sea slab has reached the uppermost mantle beneath the central part of Chugoku district [*Yamauchi et al.*, 2003; *Shiomi et al.*, 2004]. Figure 8c shows that a prominent high-velocity zone is visible from south of Shikoku to the central part of the Chugoku district, and we interpreted it to be the Philippine Sea slab. The leading edge of the Philippine Sea slab is consistent with that determined by receiver function analyses [*Shiomi et al.*, 2004; *Ramesh et al.*, 2005]. *Ochi et al.* [2001] and *Zhao et al.* [2004] suggested that the Philippine Sea slab extends further north aseismically down to a depth of 200 km under the Japan Sea. However, it remains unclear whether the slab reaches under the Japan Sea because of the insufficiency of rays to resolve the velocity structure at those locations. Beneath Kyushu, where the slab seismicity associated with the subducted Philippine Sea slab is well developed, the slab can be traced down to depths >150 km and locally to depths in excess of ~200 km (Figure 8d). The results of the CRTs are well recovered in the regions of slab seismicity, and hence the obtained images are reliable.

[22] We have delineated the upper boundary of the Philippine Sea slab from more than 40 across- and along-arc vertical cross sections with a horizontal interval of 20 km (including the figures shown hereafter) by taking into account the continuity of the high-velocity zone between adjacent cross sections. Figure 9 shows a map depicting the configuration of the upper boundary of the Philippine Sea slab thus determined. The gray and blue broken curves indicate the leading edge of the seismic [*Nakamura et al.*, 1997; *Miyoshi and Ishibashi*, 2004] and aseismic Philippine Sea slabs (this study), respectively. The geometry of the Philippine Sea slab is complicated, and the depth of the slab varies along the arc. One interesting feature is that the shallow subduction of the Philippine Sea slab beneath the Kinki district contrasts with the steeper dip beneath the Chubu district. This difference might yield a regional variation of volcanism. Most importantly, the leading edge of the Philippine Sea slab extends further north than the seismic portion of the slab. Note that although we delineate the isodepth contours of the Philippine Sea slab in northern Kyushu down to depths of 100–130 km, the occurrence of several earthquakes at a depth of ~150 km including the *M*6.2 event that occurred on 12 July 2006 (the JMA unified catalog), suggest the existence of the slab there as well.

[23] In this study, we used the upper envelope of slab earthquakes to delineate the upper boundary of the Philippine Sea slab on the basis of the assumption that slab earthquakes occur in the oceanic crust. If the slab earthquakes occur within the oceanic mantle, as observed in the eastern part of Shikoku and the western part of the Kii Peninsula [e.g., *Seno et al.*, 2001; *Shiomi et al.*, 2004], the actual upper plate interface of the Philippine Sea slab in that region would be several kilometers shallower than that inferred from the upper envelope of the seismicity. However, many of the slab earthquakes in SW Japan are interpreted as having occurred within the untransformed subducted oceanic crust [*Wang et al.*, 2004], and we consider that the upper envelope of the slab earthquakes would be a reliable indicator to represent
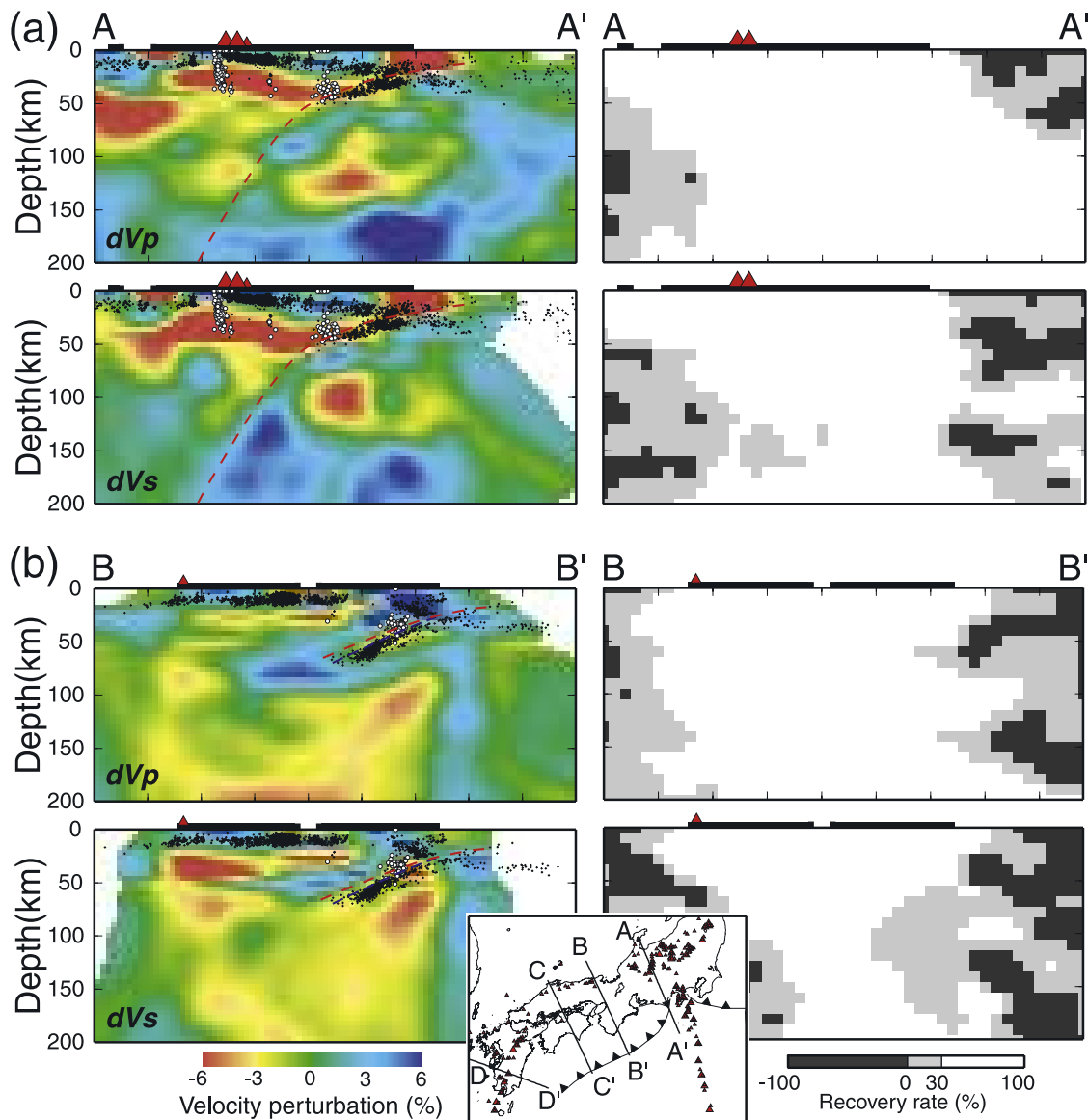
Figure 8. Across-arc vertical cross sections of the *P* and *S* wave velocity perturbations along four profiles, (a) A-A′, (b) B-B′, (c) C-C′, and (d) D-D′, in the inset map. Left upper and lower panels represent *P* and *S* wave velocity perturbations, respectively, and right panels represent the recovery rate of the CRTs for the corresponding figure. The red curve in each figure indicates the delineation of the upper boundary of the Philippine Sea slab determined in this study. Blue curves in Figures 8b and 8c indicate the oceanic Moho estimated by the receiver function analyses by *Yamauchi et al.* [2003] and *Shiomi et al.* [2004], respectively. Large and small red triangles on the top of each figure denote active and Quaternary volcanoes, respectively. Other symbols are the same as those in Figure 7.

the upper interface of the Philippine Sea slab for the entire SW Japan.

4.2. Subduction of the Philippine Sea Slab Toward the North of the Izu Peninsula

[24] The north of the Izu Peninsula is a collision zone where the Izu-Bonin ridge, an intraoceanic arc, is impinging into central Japan (Figure 1) [*Soh et al.*, 1998]. North to northeast of the Izu Peninsula is a large fan-shaped seismicity gap associated with the Philippine Sea slab. This feature is obvious in the previous configuration of the Philippine Sea slab [e.g., *Ishida*, 1992] and is also shown

in the recent high-quality hypocenter catalogue of the JMA [e.g., *Ishibashi*, 2004]. The region is also characterized by the absence of nonvolcanic low-frequency tremors [*Obara*, 2002] and the presence of Quaternary volcanoes. *Ishida* [1992] pointed out that the inclination of the slab is steeper at the Sagami trough than at the eastern end of the Nankai trough and proposed a model with the splitting of the Philippine Sea slab into two parts. *Mazzotti et al.* [1999] hypothesized the existence of the slab tear corresponding to a V-shaped seismic gap at the north of the Izu Peninsula to account for the deformation patterns observed around it.
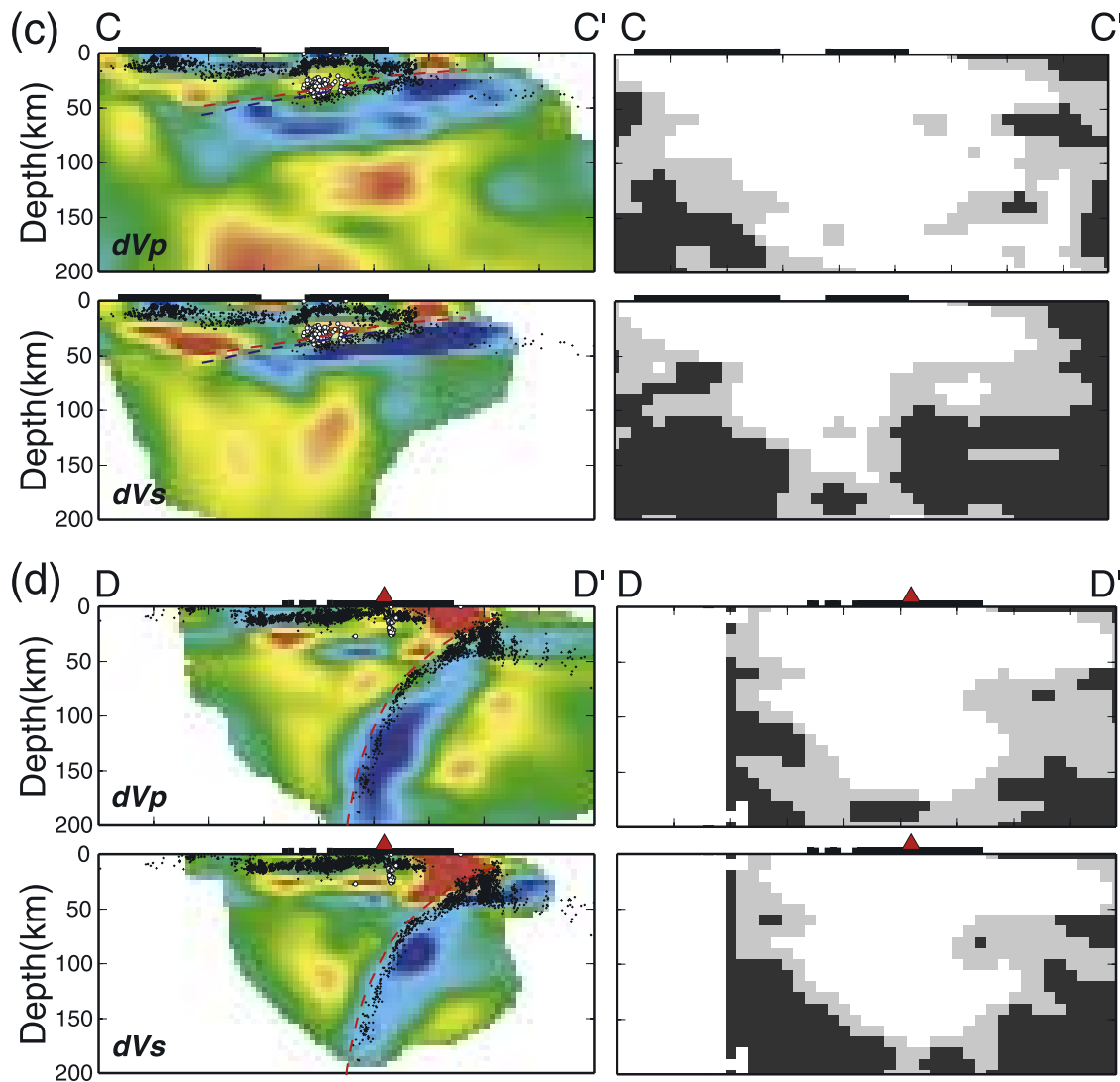
Figure 8. (continued)

[25] *Iidaka et al.* [1990] found a clear *X* phase between *P* and *S* phases on seismograms from an earthquake in the Kanto-Chubu region and interpreted the *X* phase as the *S*-to-*P* converted wave at the upper boundary of the subducting Philippine Sea plate. They deduced the subduction of the Philippine Sea slab down to a depth of 20 km even north of the Izu Peninsula. *Sekiguchi* [2001] pointed out the existence of the high-velocity zone north of the Izu Peninsula for depths >70 km with implications for the existence of the aseismic Philippine Sea slab there. *Seno and Yamasaki* [2003] argued that the lack of low-frequency tremors around the Izu Peninsula is not due to the absence of a subducted slab but due to the lack of slab dehydration because of the subduction of an island arc. *Seno* [2005] hypothesized, on the basis of recent Global Positioning System (GPS) velocities around the Izu Peninsula [*Ishibashi and Itani*, 2004], that there is a horizontal detachment at a depth of 20 km beneath the Izu Peninsula that corresponds to the interface of the Philippine Sea slab underthrusting beneath the western part of the Izu Peninsula with a dip to the north from the northern neck of the peninsula.

[26] As described above, it remains unclear whether the Philippine Sea slab is subducting north of the Izu Peninsula despite intensive studies through geophysical, geological, and geodetical approaches. Therefore it is of considerable importance to conclude whether or not the Philippine Sea slab is subducting north to northwest of the Izu Peninsula, which would enhance our understanding of the ongoing processes and the tectonics around the Izu Peninsula. Here we address the velocity structures north to northwest of the Izu Peninsula in detail.

[27] Figure 10 shows along-arc vertical cross sections of the *S* wave velocity perturbation. The red broken curves represent the upper interface of the Philippine Sea slab calculated from the isodepth contours shown in Figure 9. In the southernmost profile (Figure 10d), earthquakes associated with the Philippine Sea slab become shallower toward the neck of the Izu Peninsula, and the inferred upper interface of the Philippine Sea slab is located immediately above the slab seismicity, suggesting the validity of the configuration of the Philippine Sea slab proposed in this study. *Iidaka et al.* [1990] deduced the subduction of the Philippine Sea slab down to a depth of 20 km in this region,
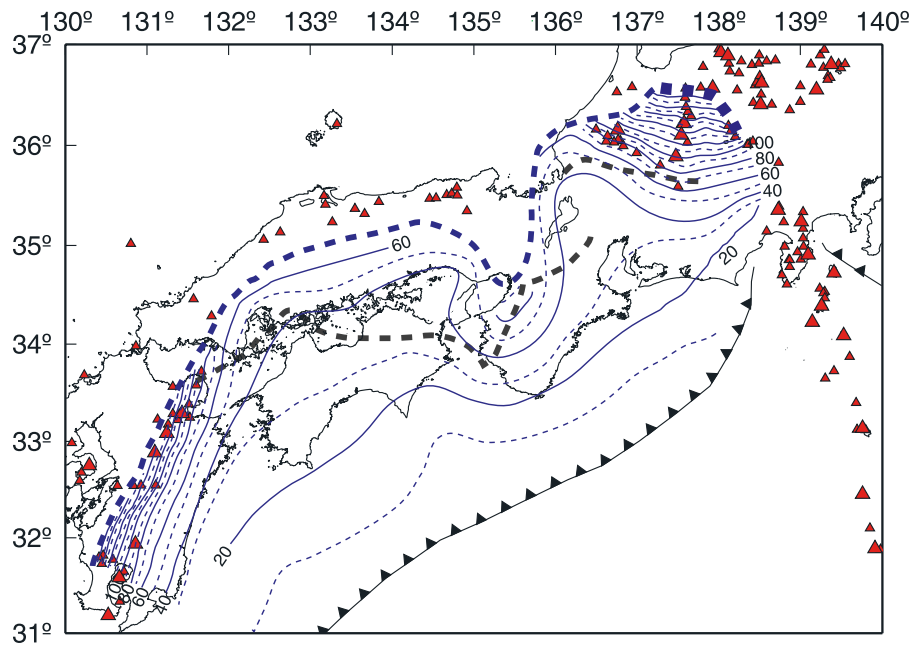
Figure 9. Depth contour map of the upper boundary of the Philippine Sea slab with an interval of 10 km obtained in this study. Gray broken curves indicate the leading edge of the Philippine Sea slab inferred from the seismicity [*Nakamura et al.*, 1997; *Miyoshi and Ishibashi*, 2004], while a blue broken curve represents the leading edge of the Philippine Sea slab obtained in this study. Except for Kyushu, the blue broken curve corresponds to the leading edge of the aseismic Philippine Sea slab. A thick dark blue curve along the leading edge in central Japan denotes the region where the Philippine Sea slab might have collided with the Pacific slab (see text for details). Note that the isodepth contours of 10 and 20 km are taken from *Baba et al.* [2002], in which the upper boundary of the Philippine Sea slab is estimated from reflection/refraction surveys. Large and small red triangles denote active and Quaternary volcanoes, respectively.

which supports the shallow subduction of the Philippine Sea slab at the neck of the Izu Peninsula.

[28] In Figure 10c, the earthquakes associated with the Philippine Sea slab are visible in the western part of the profile in the depth range of 30–70 km, and the high-velocity zone exists below the seismicity. A prominent high-velocity zone is also imaged immediately above the Pacific slab east of the Izu Peninsula in a horizontal distance of 350 km; this zone corresponds to the Philippine Sea slab subducted from the Sagami trough [e.g., *Ishida*, 1992] or a detached piece of the slab (disclosed fragment block) [*Toda et al.*, 2005]. Although the amplitude of the high-velocity zone appears to be weak below the volcanic front, the high-velocity zone could be traced continuously from west to east across the north of the Izu Peninsula at depths of 70–80 km. The continuity of the high-velocity zone is also evident in the map view of the velocity structures in Figure 6, in particular for the *P* wave, suggesting subduction of the Philippine Sea slab even north of the Izu Peninsula. The checkerboard patterns are well recovered in the region, and we consider that the high-velocity zone imaged at depths of 70–80 km is reliable and robust. The weak high-velocity anomaly might be attributable to the inherent warm nature of the slab due to the subduction of the Izu-Bonin volcanic ridge. In addition, it is likely that the subducted fossil volcanic ridge would possibly contain fracture zones and/or conduits through which fluids derived from the Pacific slab had migrated

upward and formed volcanoes on the Philippine Sea plate prior to its subduction, which have also contributed to lower the seismic velocity. We infer that fluids derived from the Pacific slab could partly migrate upward through fractures/conduits within the Philippine Sea slab and cause volcanic activity at the surface.

[29] In Figure 10a, the seismicity associated with the Philippine Sea slab shows that the Philippine Sea slab is almost horizontal at depths of 40–50 km in the western part of the profile. We interpret an eastward-dipping high-velocity zone that continues from the seismic Philippine Sea slab to be the aseismic Philippine Sea slab. The inclination of the aseismic slab becomes steeper toward the east, and the Philippine Sea slab finally reaches the Pacific slab at the northwestern extension of the Izu Peninsula, as indicated by the red curve. The Philippine Sea slab subducted from the Sagami trough exists above the Pacific slab at a horizontal distance of ∼350 km. It appears that the Philippine Sea slab is not continuous at horizontal distances of 250–300 km in Figure 10a, suggestive of an offset of the slab. The subduction of the Izu-Bonin volcanic ridge might have weakened the strength of the slab and caused the tear along it. The western part of the split Philippine Sea slab might have sunk because of its negative buoyancy and collided with the Pacific slab at depths of 150–200 km.

[30] The transition from the continuous to discontinuous Philippine Sea slab is shown in Figure 10b. The seismicity *X* is isolated and considered to occur in the deepest portion
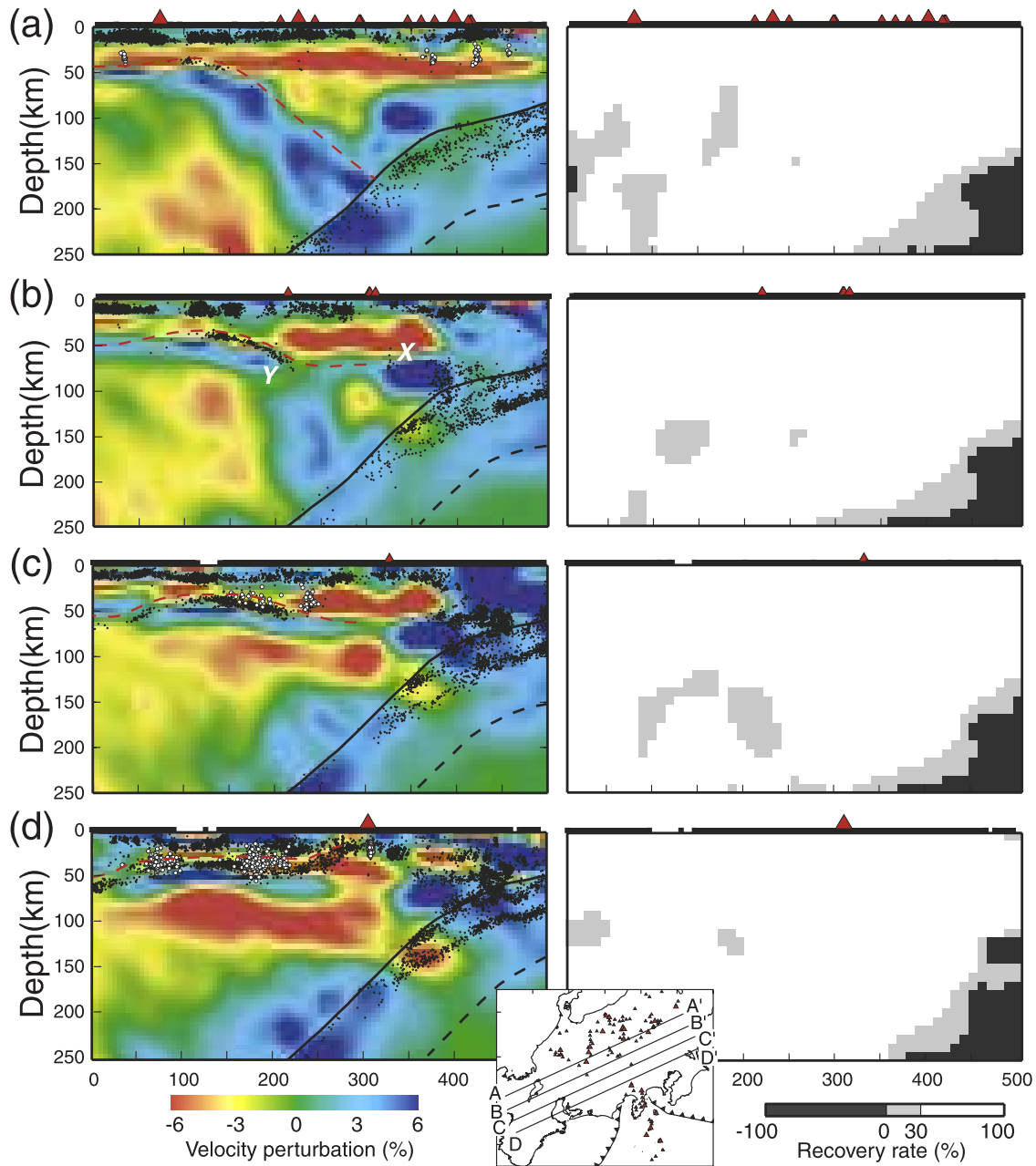
Figure 10. Along-arc vertical cross sections of (left) S wave velocity perturbations and (right) the recovery rate of the CRTs along four profiles, (a) A-A′, (b) B-B′, (c) C-C′, and (d) D-D′, in the inset map. All cross sections intersect the north of the Izu collision zone. The red broken curves are the upper boundary of the Philippine Sea slab derived from the isodepth contours shown in Figure 9. Labels of X and Y in Figure 10b represent the seismicity discussed in the text. Solid curves denote the upper interface of the Pacific slab adopted in the inversion [*Zhao and Hasegawa*, 1993; *Nakajima and Hasegawa*, 2006]. Other symbols are the same as those in Figures 7 and 8.

of the Philippine Sea slab subducted beneath the Kanto district [e.g., *Sekiguchi*, 2001; *Nakamura et al.*, 2002], while the inclined seismicity Y is considered to be associated with the Philippine Sea slab subducted beneath the Chubu district. Considering the continuity of the high-velocity zone between adjacent cross sections, the Philippine Sea slab is estimated to lie along the red broken curve so as to connect the two seismicities. However, it might be possible to interpret that the Philippine Sea slab droops over the Pacific

slab along a steeper inclination of the seismicity Y. In any case, the configuration of the Philippine Sea slab changes abruptly between lines A-A′ and B-B′.

[31] The thick dark blue broken curve in Figure 9 indicates the spatial extent of the area where the Philippine Sea slab might have collided with the Pacific slab. If two slabs are colliding, the stress regime in that region could be disturbed; the focal mechanism of intraslab earthquakes could be used to test this possibility. However, few focal
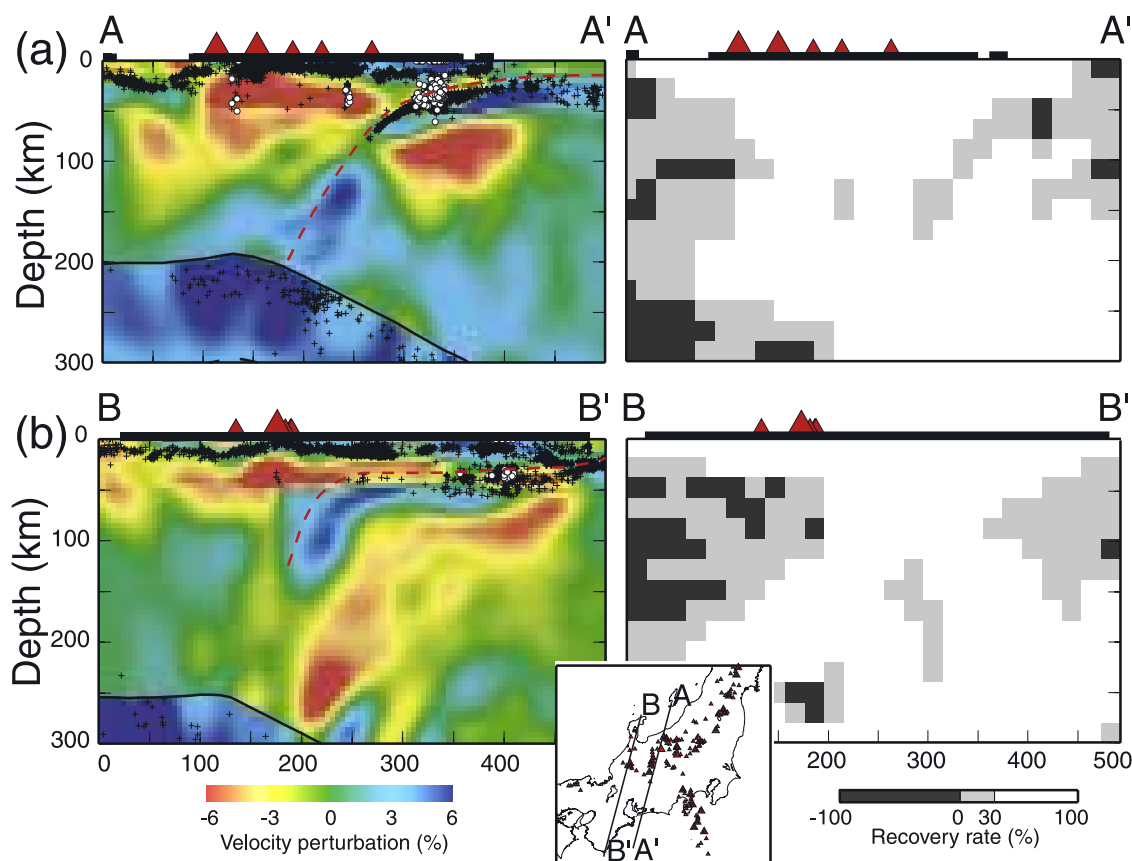
Figure 11. Vertical cross sections of (left) *S* wave velocity perturbations and (right) the recovery rates of the CRTs along two profiles, (a) A-A′ and (b) B-B′, in the inset map. Other symbols are the same as those in Figures 7 and 8.

mechanisms have been determined by the JMA around the region because of the occurrence of earthquakes at deeper depths. A detailed investigation of focal mechanisms of earthquakes around the collision zone will help us to understand the ongoing physical processes in a unique tectonic setting of the collision of the two slabs.

4.3. Role of the Philippine Sea Slab on Volcanism in Central Japan

[32] As the Philippine Sea slab is subducted beneath SW Japan and overlapping the older Pacific slab, the upper mantle structure and arc magmatism are likely to have been affected. We consider three possible effects of the Philippine Sea slab on the arc magmatism. One is to shift the dehydration reactions in the Pacific slab to a greater depth because the presence of the cold Philippine Sea slab prevents the Pacific slab from heating normally [*Iwamori*, 2000]. The second is to act as a barrier to fluids rising from the Pacific slab, and the third is to release the fluids to the mantle from dehydration of minerals within the Philippine Sea slab itself.

[33] Previous studies have investigated volcanism in the Kyushu and Chugoku districts through geochemical, geological, and geophysical approaches, and conceptual models of volcanism have been proposed. Briefly, a clear volcanic front is present in the Kyushu district, and the fluids from the Philippine Sea slab are considered to be important for volcanism along the volcanic front [e.g., *Kamata*, 1998; *Zhao et al.*, 2000; *Wang and Zhao*, 2006b]. The back-arc

volcanism in Kyushu is responsible for the extensive mantle upwelling associated with the opening of the Okinawa trough along the eastern Asian margin during the Cenozoic [e.g., *Nakada et al.*, 1997]. For the Chugoku district, primary magmas originating from the upper mantle play an important role in Quaternary volcanism [*Iwamori*, 1992]. As the leading edge of the Philippine Sea slab considered in this study has not reached the region below the Quaternary volcanoes in the Chugoku district (Figure 9), the subducted Philippine Sea slab cannot act as the fundamental source of magma for volcanoes in this region. *Nakajima and Hasegawa* [2007] revealed a large low-velocity anomaly in the upper mantle beneath the Chugoku district and interpreted it to be a mantle upwelling. They also argued that the mantle upwelling reaches the uppermost mantle passing through the north of the leading edge of the Philippine Sea slab, forming a line-shaped distribution of Quaternary volcanoes along the coastline of the Japan Sea in the Chugoku district.

[34] There are two remarkable features of volcanism in central Japan. One is the deflection of the volcanic front to the back-arc region, and the other is the concentration and absence of volcanoes in the Chubu and Kinki districts, respectively. The deflection of the volcanic front is considered to be caused by the subduction of the Philippine Sea plate beneath the region from the Sagami and the eastern end of the Nankai troughs. *Iwamori* [2000] showed through numerical simulations that the thermal recovery of the

subducting Pacific plate is slow because of the overlapping Philippine Sea plate, which shifts the dehydration reactions to greater depths along the Pacific plate. In fact, Figure 6 shows that the low-velocity zone exists along the volcanic front at a depth of 40 km, except beneath the Kanto district, which is interpreted as an oceanic crust of the subducted Philippine Sea slab [*Matsubara et al.*, 2005]. At depths of 60 and 80 km, the low-velocity zone deflects toward the back arc, corresponding to the deflection of the volcanic front. These observations confirm the validity of the interpretation by *Iwamori* [2000].

[35] Figure 11 depicts the vertical cross sections of the *S* wave velocity perturbations along two profiles in the insert map. Figure 11a shows that the Philippine Sea slab is subducting seismically at a low dip to a depth of 80 km

and then bends downward and is aseismic at greater depths. The Philippine Sea slab reaches the subducted Pacific slab at a depth of ∼200 km. The high-velocity anomaly is weak near the downward bend, as pointed out by *Honda and Nakanishi* [2003]. A high-velocity zone corresponding to the aseismic Philippine Sea slab is also traced down to a depth of ∼130 km in Figure 11b. The Philippine Sea slab extends south of the volcanic area. Volcanoes have formed only in the region where the Philippine Sea slab is subducting at a higher dip. This feature is clearly seen in the cross section of Figure 10a and in the isodepth contours of Figure 9.

[36] Although the supply of fluids from the Pacific slab is an important factor to induce arc magmatism, as suggested by *Iwamori* [2000], we consider that the geometry of the subducted Philippine Sea slab has another crucial effect on the surface manifestation of volcanoes in central Japan. As described above, it is evident that the volcanoes in central Japan have formed in the region below which the Philippine Sea slab is subducting at a higher dip, whereas no volcanism occurs above the shallowly subducting portion of the Philippine Sea slab. In addition, volcanoes in the Norikura Volcanic Chain [e.g., *Kimura and Yoshida*, 1999] are distributed sub-parallel to the local dip direction of the subducted Philippine Sea slab (Figure 12a). The spatial correspondence between the configuration of the Philippine Sea slab and the surface manifestation of volcanoes suggests the important role of the Philippine Sea slab on volcanism in central Japan.

[37] For the young Philippine Sea slab, dehydration reactions in the slab mostly occur before reaching a depth of ∼50 km [e.g., *Peacock and Wang*, 1999; *Yamasaki and Seno*, 2003; *Hacker et al.*, 2003]. The occurrence of nonvolcanic deep tremors [*Obara*, 2002] at depths of 30–40 km is one of the indicators of significant dehydration from the oceanic crust. Consequently, hydrous minerals such as chlorite and serpentine could be formed at the base
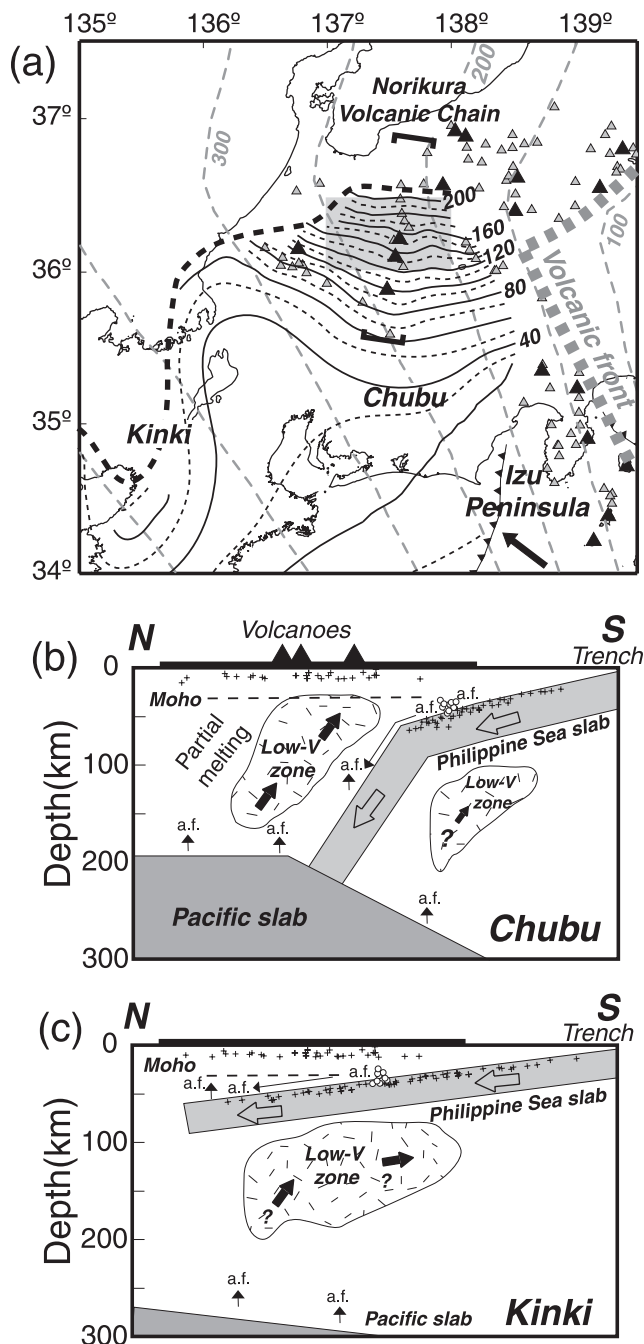

Figure 12. (a) Map showing the distribution of volcanoes together with the isodepth contours of the Philippine Sea slab with an interval of 10 km. Black and gray triangles denote active and Quaternary volcanoes, respectively. The volcanic front is represented by a thick gray broken curve. The plate motion of the Philippine Sea slab relative to the overriding plate is shown by a gray arrow [*Seno et al.*, 1996]. The isodepth contours of the Pacific slab are shown by the gray-broken curves with an interval of 50 km [*Zhao and Hasegawa*, 1993; *Nakajima and Hasegawa*, 2006]. The Norikura Volcanic Chain [e.g., *Kimura and Yoshida*, 1999] discussed in the text is labeled. A gray rectangle indicates the region where the anisotropy with a symmetry axis is oriented N20°E [*Hiramatsu et al.*, 1998]. Schematic illustrations of the north-south vertical cross sections of (b) Chubu and (c) Kinki regions. Crosses and white circles denote microearthquakes and deep low-frequency tremors, respectively. Possible sources of aqueous fluids (a.f.) are shown by arrows. Partial melting might have occurred in the low-velocity zone in the mantle wedge, which is the source of magmas for volcanoes. The subhorizontal subduction of the Philippine Sea slab prevents the magma from upwelling to the uppermost mantle, as shown in Figure 12c.

of the overlying mantle wedge. These hydrous minerals could be dragged down to deeper regions by the subduction of the Philippine Sea slab, accompanied by a mantle return flow. The release of fluids to the overlying mantle wedge at greater depths would initiate melting there. The generated melts would then be transported to the uppermost mantle through the return flow, causing arc volcanism at the surface [e.g., *Nakajima et al.*, 2001; *Hasegawa and Nakajima*, 2004].

[38] The distribution of volcanoes in central Japan could be explained as follows. The subduction of the Philippine Sea slab at a steep dip could induce an effective mantle return flow such that fluids and/or melts are efficiently transported to the uppermost mantle and act as magma sources for volcanoes. The low-velocity zone imaged above the Philippine Sea slab in central Japan may be attributable to such fluids/melts (Figure 12b). Shear wave splitting measurements detected an anisotropic body with a symmetry axis oriented N20°E only around the Norikura Volcanic Chain (a gray rectangle in Figure 12a) [e.g., *Ando et al.*, 1983; *Hiramatsu et al.*, 1998]. The depth of the anisotropic body ranges from 100 to 180 km [*Hiramatsu et al.*, 1998], roughly consistent with the low-velocity zone above the Philippine Sea slab (Figure 11a). The anisotropy due to the lattice-preferred orientation of olivine induced by the mantle return flow could be subparallel to the maximum-dip direction of the slab [*Nakajima et al.*, 2006], which could account for the observed shear wave splitting.

[39] The subhorizontal subduction of the slab has two possible negative effects on arc magmatism. The subduction of the Philippine Sea slab at a shallow dip is incapable of inducing an effective mantle upwelling. This in turn does not inhibit mantle wedge melting, even if the fluids are released to the mantle wedge from the Philippine Sea slab. Another effect is that the subhorizontal subduction of the Philippine Sea slab could act as a barrier to fluids upwelling from the Pacific slab. When the fluids associated with the Pacific slab are released to the mantle wedge by the breakdown of phase A at a depth >300 km in central Japan [*Iwamori*, 2000], the existence of the subhorizontal slab prevents the fluids and/or melts from ascending to the uppermost mantle. The favored interpretation is that the absence of volcanoes in the Kinki district might be attributable to these negative effects of the subhorizontal subduction of the Philippine Sea slab (Figure 12c). A prominent low-velocity zone imaged below the subducted Philippine Sea slab may reflect the accumulation of fluids and/or melts derived from the Pacific slab.

5. Conclusions

[40] This paper reveals the detailed three-dimensional seismic velocity structure beneath SW Japan and determines the configuration of the Philippine Sea slab using recent high-quality arrival-time data. This study yields new insight into the tectonic framework in SW Japan, in terms of the subduction of the Philippine Sea slab.

[41] 1. The subduction of the aseismic Philippine Sea slab is revealed at the deeper extension of the seismic slab in SW Japan except for the Kyushu region. The inferred slab geometry is complicated and varies along the arc. The Philippine Sea slab is subducting at least down to a depth

of 200 km in Chubu, 60–80 km in Kinki, 60 km in Chugoku, and 150–200 km in Kyushu.

[42] 2. The Philippine Sea slab is subducting toward the north to northwest of the Izu Peninsula down to a depth of ~70 km, whereas the slab appears to split into the eastern and western parts at greater depths. The Philippine Sea slab split into the western part might have reached the Pacific slab at a depth of ~200 km at the northwest extension of the Izu Peninsula with implications for the collision of the two oceanic slabs. The splitting might have occurred along the subducted Izu-Bonin volcanic ridge.

[43] 3. The concentration and absence of volcanoes in the Chubu and Kinki districts, respectively, are attributable to the difference in a subduction angle of the Philippine Sea slab. The subduction of the Philippine Sea slab at a low dip could not induce sufficient mantle upwelling to generate arc magmas. The subhorizontal subduction of the Philippine Sea slab could prevent the mantle upwelling induced by the subduction of the Pacific slab from ascending to the uppermost mantle. In contrast, subduction at a high dip could effectively induce the mantle return flow and facilitate the migration of fluids and/or melts to the uppermost mantle.

[44] The modeling of subduction-zone processes by incorporating the aseismic Philippine Sea slab and comprehensive seismological studies including attenuation tomography and shear wave splitting measurements are required for a better understanding of the tectonics in SW Japan. A detailed and small-scale configuration of the shallower part of the slab is also important to model the occurrence of megathrust earthquakes such as the Nankai and Tonankai earthquakes. The detailed analyses of these and other possible subjects are left open for future studies.

References

Ando, M., Y. Ishikawa, and F. Yamazaki (1983), Shear wave polarization anisotropy in the upper mantle beneath Honshu Japan, *J. Geophys. Res.*, *88*, 5850–5864.

Baba, T., Y. Tanioka, P. R. Cummins, and K. Uhira (2002), The slip distribution of the 1946 Nankai earthquake estimated from tsunami inversion using a new plate model, *Phys. Earth Planet. Inter.*, *132*, 59–73.

Committee for Catalog of Quaternary Volcanoes in Japan (1999), Catalog of Quaternary volcanoes in Japan, ver.1.0, Volcanological Society of Japan.

Goto, K., T. Honda, H. Yakiwara, T. Kakuta, and H. Shimizu (2001), Geometry and focal mechanisms of moderately deep seismic zone beneath southern Kyushu (in Japanese), *Chikyu Mon.*, *23*, 664–668.

Hacker, B. R., S. M. Peacock, G. A. Abers, and S. D. Holloway (2003), Subduction factory 2. Are intermediate-depth earthquakes in subducting

slabs linked to metamorphic dehydration reactions?, *J. Geophys. Res.*, *108*(B1), 2030, doi:10.1029/2001JB001129.

Hasegawa, A., and J. Nakajima (2004), Geophysical constraints on slab subduction and arc magmatism, in *The State of the Planet: Frontiers and Challenges in Geophysics*, *Geophys. Monogr. Ser.*, vol. 150, pp. 81–94, AGU, Washington, D.C.

Headquarters for Earthquake Research Promotion (2001), On the long-term evaluation of earthquakes in the Nankai Trough (in Japanese), http://www.jishin.go.jp/main/chousa/01sep_nankai/index.htm.

Hiramatsu, Y. M. Ando, T. Tsukuda, and T. Ooida (1998), Three-dimensional image of the anisotropic bodies beneath central Honshu, Japan, *Geophys. J. Int.*, *135*, 801–816.

Hirose, H., and K. Obara (2005), Repeating short- and long-term slow slip events with deep tremor activity around Bungo channel region, southwest Japan, *Earth Planets Space*, *57*, 961–972.

Honda, S., and I. Nakanishi (2003), Seismic tomography of the upper-most mantle beneath southwestern Japan: Seismological constraints on modeling subduction and magmatism for the Philippine Sea slab, *Earth Planets Space*, *55*, 443–462.

Hori, S. (2006), Seismic activity associated with the subducting motion of the Philippine Sea plate beneath the Kanto district Japan, *Tectonophysics*, *417*, 85–100.

Hori, S., H. Inoue, Y. Fukao, and M. Ukawa (1985), Seismic detection of the untransformed "basaltic" oceanic crust subducting into the mantle, *Geophys. J. R. Astron. Soc.*, *83*, 169–197.

Iidaka, T., M. Mizoue, I. Nakamura, T. Tsukuda, K. Sakai, M. Kobayasi, T. Haneda, and S. Hashimoto (1990), The upper boundary of the Philippine sea plate beneath the western Kanto region estimated from S–P-converted wave, *Tectonophysics*, *179*, 321–326.

Iidaka, T., T. Iwasaki, T. Takeda, T. Moriya, I. Kumakawa, E. Kurashimo, T. Kawamura, F. Yamasaki, K. Koike, and G. Aoki (2003), Configuration of subducting Philippine Sea plate and crustal structure in the central Japan region, *Geophys. Res. Lett.*, *30*(5), 1219, doi:10.1029/2002GL016517.

Ishibashi, K. (2004), Seismotectonic modeling of the repeating M7-class disastrous Odawara earthquake in the Izu collision zone, central Japan, *Earth Planets Space*, *56*, 843–858.

Ishibashi, K., and Y. Itani (2004), Explanation of the westward motion of the Izu Peninsula by collision—An interpretation of GPS velocity vectors-(in Japanese with English abstract), *J. Seismol. Soc. Japan*, *35*, 195–212.

Ishida, M. (1992), Geometry and relative motion of the Philippine Sea plate and Pacific plate beneath the Kanto-Tokai district Japan, *J. Geophys. Res.*, *97*, 453–489.

Iwamori, H. (1992), Degree of melting and source composition of Cenozoic basalts in southwest Japan: Evidence for mantle upwelling by flux melting, *J. Geophys. Res.*, *97*, 10,983–10,995.

Iwamori, H. (2000), Deep subduction of H2O and deflection of volcanic chain towards backarc near triple junction due to lower temperature, *Earth Planet. Sci. Lett.*, *181*, 41–61.

Kamata, H. (1998), Quaternary volcanic front at the junction of Southwest Japan Arc and the Ryukyu Arc, *Asian Earth Sci.*, *16*, 67–75.

Katsumata, A., and N. Kamaya (2003), Low-frequency continuous tremor around the Moho discontinuity away from volcanoes in the southwest Japan, *Geophys. Res. Lett.*, *30*(1), 1020, doi:10.1029/2002GL015981.

Kimura, J., and T. Yoshida (1999), Magma pluming system beneath Ontake Volcano, central Japan, *Isl. Arc*, *8*, 1–29.

Kimura, J., R. J. Stern, and T. Yoshida (2005), Reinitiation of subduction and magmatic responses in SW Japan during Neogene time, *GSA Bull.*, *117*, 969–986.

Kimura, H., K. Kasahara, T. Igarashi, and N. Hirata (2006), Repeating earthquake activities associated with the Philippine Sea plate subduction in the Kanto district, central Japan: A new plate configuration revealed by interplate seismic slips, *Tectonophysics*, *417*, 101–118.

Kodaira, S., T. Iidaka, A. Kato, J. O. Park, T. Iwasaki, and Y. Kaneda (2004), High pore fluid pressure may cause silent slip in the Nankai trough, *Science*, *304*, 1295–1298.

Matsubara, M., H. Hayashi, K. Obara, and K. Kasahara (2005), Low-velocity oceanic crust at the top of the Philippine Sea and Pacific plates beneath the Kanto region, central Japan, imaged by seismic tomography, *J. Geophys. Res.*, *110*, B12304, doi:10.1029/2005JB003673.

Mazzotti, S., P. Henry, X. L. Pichon, and T. Sagiya (1999), Strain partitioning in the zone of transition from Nankai subduction to Izu-Bonin collision (central Japan): implications for an extensional tear within the subducting slab, *Earth Planet. Sci. Lett.*, *172*, 1–10.

Miyoshi, T., and K. Ishibashi (2004), Geometry of the Seismic Philippine Sea slab beneath the region from Ise Bay to western Shikoku, southwest Japan (in Japanese with English abstract), *J. Seismol. Soc. Japan*, *57*, 139–152.

Nakajima, J., and A. Hasegawa (2006), Anomalous low-velocity zone and linear alignment of seismicity along it in the subducted Pacific slab

beneath Kanto, Japan: Reactivation of subducted fracture zone?, *Geophys. Res. Lett.*, *33*, L16309, doi:10.1029/2006GL026773.

Nakajima, J., and A. Hasegawa (2007), Tomographic evidence for the mantle upwelling beneath southwestern Japan and its implications for arc magmatism, *Earth Planet. Sci. Lett.*, *254*, 90–105.

Nakajima, J., T. Matsuzawa, A. Hasegawa, and D. Zhao (2001), Three-dimensional structure of Vp, Vs, and Vp/Vs beneath northeastern Japan: Implications for arc magmatism and fluids, *J. Geophys. Res.*, *106*, 21,843–21,857.

Nakajima, J., J. Shimizu, S. Hori, and A. Hasegawa (2006), Shear-wave splitting beneath the southwestern Kurile arc and northeastern Japan arc: A new insight into mantle return flow, *Geophys. Res. Lett.*, *33*, L05305, doi:10.1029/2005GL025053.

Nakamura, M., H. Watanabe, T. Konomi, S. Kimura, and K. Miura (1997), Characteristic activities of subcrustal earthquakes along the outer zone of southwestern Japan (in Japanese with English abstract), *Ann. Disast. Prev. Res. Inst., Kyoto Univ.*, *40*, 1–20.

Nakamura, M., et al. (2002), Three-dimensional *P* and *S* wave velocity structure beneath central Japan (in Japanese with English abstract), *Pap. Meteorol. Geophys.*, *53*, 1–28.

Nakanishi, I. (1980), Precursors to ScSp phases and dipping interface in the upper mantle beneath southwestern Japan, *Tectonophysics*, *69*, 1–35.

Nakanishi, I., Y. Kinoshita, and K. Miura (2002), Subduction of young plates: A case of the Philippine Sea slab beneath the Chugoku region, Japan, *Earth Planets Space*, *54*, 3–8.

Nakamura, M., T. Yanagi, and S. Maeda (1997), Lower crustal erosion induced by mantle diapiric upwelling: Constraints from sedimentary basin formation followed by voluminous basalt volcanism in northwest Kyushu Japan, *Earth Planet. Sci. Lett.*, *146*, 415–429.

Obara, K. (2002), Nonvolcanic deep tremor associated with subduction in southwest Japan, *Science*, *296*, 1679–1681.

Ochi, F., M. Nakamura, and D. Zhao (2001), Deep structure of the subducting Philippine Sea slab under southwestern Japan (in Japanese), *Earth Mon.*, *23*, 679–684.

Oda, H., and T. Douzen (2001), New evidence for a low-velocity layer on the subducting Philippine Sea plate in southwest Japan, *Tectonophysics*, *332*, 347–358.

Ohkura, T. (2000), Structure of the upper part of the Philippine Sea plate estimated by later phases of upper mantle earthquakes in and around Shikoku, Japan, *Tectonophysics*, *321*, 17–36.

Okada, Y., K. Kasahara, S. Hori, K. Obara, S. Sekiguchi, H. Fujiwara, and A. Yamamoto (2004), Recent progress of seismic observation networks in Japan -Hi-net, F-net, K-NET and KiK-net -, *Earth, Planets Space*, *56*, xv–xviii.

Okino, K., Y. Shimakawa, and S. Nagaoka (1994), Evolution of the Shikoku Basin, *J. Geomagn. Geoelectr.*, *46*, 279–463.

Ozawa, S., M. Murakami, M. Kaidzu, T. Tada, T. Sagiya, Y. Hatanaka, H. Yarai, and T. Nishimura (2002), Detection and monitoring of ongoing aseismic slip in the Tokai region, central Japan, *Science*, *298*, 1009–1012.

Peacock, S. M., and K. Wang (1999), Seismic consequences of warm versus cool subduction metamorphism: Examples from southwest and northeast Japan, *Science*, *286*, 937–939.

Ramesh, D. S., H. Kawakatsu, S. Watada, and X. Yuan (2005), Receiver function images of the central Chugoku region in the Japanese islands using Hi-net data, *Earth Planets Space*, *57*, 271–280.

Salah, M. K., and D. Zhao (2003), 3-D seismic structure of Kii Peninsula in southwest Japan: Evidence for slab dehydration in the forearc, *Tectonophysics*, *364*, 191–213.

Sano, Y., N. Takahara, and T. Seno (2006), Geographical distribution of 3He/4He in the Chugoku district, southwestern Japan, *Pure Appl. Geophys.*, *163*, 745–767.

Sato, H., et al. (2005), Earthquake source fault beneath Tokyo, *Science*, *309*, 462–464.

Sekiguchi, S. (2001), A new configuration and a seismic slab of the descending Philippine Sea plate revealed by seismic tomography, *Tectonophysics*, *341*, 19–32.

Seno, T. (2005), Izu detachment hypothesis: A proposal of a unified cause for the Miyake–Kozu event and the Tokai slow event, *Earth Planets Space*, *57*, 925–934.

Seno, T., and T. Yamasaki (2003), Low-frequency tremors, intraslab and interplate earthquakes in southwest Japan- From a view point of slab dehydration, *Geophys. Res. Lett.*, *30*(22), 2171, doi:10.1029/2003GL018349.

Seno, T., T. Sakurai, and S. Stein (1996), Can the Okhotsk plate be discriminated from the North American plate?, *J. Geophys. Res.*, *101*, 11,305–11,315.

Seno, T., D. Zhao, Y. Kobayashi, and M. Nakamura (2001), Dehydration of serpentinized slab mantle: Seismic evidence from southwest Japan, *Earth Planets Space*, *53*, 861–871.

Shiomi, K., H. Sato, K. Obara, and M. Ohtake (2004), Configuration of subducting Philippine Sea plate beneath southwest Japan revealed from receiver function analysis based on the multivariate autoregressive model, *J. Geophys. Res.*, *109*, B04308, doi:10.1029/2003JB002774.

Soh, W., K. Nakamura, and T. Kimura (1998), Arc–arc collision in the Izu collision zone, central Japan, deduced from the Ashigara Basin and adjacent Tanzawa Mountains, *Isl. Arc*, *7*, 330–341.

Toda, S., R. S. Stein, S. B. Bozkurt, and R. Nakamura (2005), A dislodged tectonic block wedged beneath Tokyo, and implications for the enigmatic 1855 Ansei-Edo Earthquake, *Eos Trans. AGU*, *86*(52), Fall Meet. Suppl., Abstract, S21A-0199.

Tokuyama, H. (1995), Origin and development of the Philippine Sea, in *Geology and Geophysics of the Philippine Sea*, pp.155–163, edited by H. Tokuyama, et al., Terrapub, Tokyo.

Ueno, H., S. Hatakeyama, T. Aketagawa, J. Funaski, and N. Hamada (2002), Improvement of hypocenter determination procedures in the Japan Meteorological Agency (in Japanese), *Q. J. Seismol.*, *65*, 123–134.

Um, J., and C. Thurber (1987), A fast algorithm for two-point seismic ray tracing, *Bull. Seismol. Soc. Am.*, *77*, 972–986.

Wang, Z., and D. Zhao (2006a), Suboceanic earthquake location and seismic structure in the Kanto district, central Japan, *Earth Planet. Sci. Lett.*, *241*, 789–803.

Wang, Z., and D. Zhao (2006b), Vp and Vs tomography of Kyushu, Japan: New insight into arc magmatism and forearc seismotectonics, *Phys. Earth Planet. Inter.*, *157*, 269–285.

Wang, K., I. Wada, and Y. Ishikawa (2004), Stress in the subducting slab beneath southwest Japan and relation with plate geometry, tectonic forces, slab dehydration, and damaging earthquakes, *J. Geophys. Res.*, *109*, B08304, doi:10.1029/2003JB002888.

Wessel, P., and W. H. F. Smith (1998), New, improved version of the Generic Mapping Tools released, *Eos Trans. AGU*, *79*, 579.

Yamasaki, T., and T. Seno (2003), Double seismic zone and dehydration embrittlement of the subducting slab, *J. Geophys. Res.*, *108*(B4), 2212, doi:10.1029/2002JB001918.

Yamauchi, M., K. Hirahara, and T. Shibutani (2003), High resolution receiver function imaging of the seismic velocity discontinuities in the crust and the uppermost mantle beneath southwest Japan, *Earth Planets Space*, *55*, 59–64.

Zhao, D., and A. Hasegawa (1993), *P*-wave tomographic imaging of the crust and upper mantle beneath the Japan Islands, *J. Geophys. Res.*, *98*, 4333–4353.

Zhao, D., A. Hasegawa, and S. Horiuchi (1992a), Tomographic imaging of *P* and *S* wave velocity structure beneath northeastern Japan, *J. Geophys. Res.*, *97*, 19,909–19,928.

Zhao, D., S. Horiuchi, and A. Hasegawa (1992b), Seismic velocity structure of the crust beneath the Japan Islands, *Tectonophysics*, *212*, 289–301.

Zhao, D., A. Hasegawa, and H. Kanamori (1994), Deep structure of Japan subduction zone as derived from local, regional, and teleseismic events, *J. Geophys. Res.*, *99*, 22,313–22,329.

Zhao, D., K. Asamori, and H. Iwamori (2000), Seismic structure and magmatism of the young Kyushu subduction zone, *Geophys. Res. Lett.*, *27*, 2057–2060.

Zhao, D., H. Tani, and O. P. Mishra (2004), Crustal heterogeneity in the 2000 western Tottori earthquake region: Effect of fluids from slab dehydration, *Phys. Earth Planet. Inter.*, *145*, 161–177.

————————————

A. Hasegawa and J. Nakajima, Research Center for Prediction of Earthquakes and Volcanic Eruptions, Graduate School of Science, Tohoku University, Sendai 980-8578, Japan. (nakajima@aob.geophys.tohoku.ac.jp)